Pyrimido-Pyrimidines: A Novel Class of Dihydrofolate Reductase Inhibitors

Mihailo Banjanac[1], Iva Tatic[1], Zrinka Ivezic[2], Sanja Tomic[3] and Jerka Dumic[4]*

[1]CEMDD, GlaxoSmithKline Research Centre Zagreb, Prilaz baruna Filipovića 29, HR-10000 Zagreb, Croatia

[2]Nabriva Therapeutics AG, Leberstrasse 20, AT-1112 Vienna, Austria

[3]Physical Chemistry Department, Ruđer Bošković Institute, Bijenička cesta 54, HR-10000 Zagreb, Croatia

[4]Department of Biochemistry and Molecular Biology, Faculty of Pharmacy and Biochemistry, University of Zagreb, Ante Kovačića 1, HR-10000 Zagreb, Croatia

Summary

Inhibitors of dihydrofolate reductase (DHFR), an enzyme that catalyzes 5,6,7,8-tetrahydrofolate synthesis, have been used as antimicrobial as well as antimetabolite drugs for a long time. Although structurally belonging to different classes, the majority of DHFR inhibitors contain 2,4-diamino substitution in pyrimidine ring. With the aim to introduce pyrimido-pyrimidines as a novel class of bacterial DHFR (bDHFR) inhibitors, 42 compounds belonging to that class have been tested and compared with 18 pteridines using cell and enzyme models and docking studies. A few pyrimido-pyrimidine compounds showed high potency (IC$_{50}\leq$0.05 µM) and selectivity as inhibitors of bDHFR. These properties seem to be dependent on the stringent structure freedom and flexibility, based on the specific combination of prerequisite structural motifs that enable pyrimido-pyrimidine compounds to fit into bDHFR active site in a relatively specific manner. The presented results will help to set the basis for designing new small molecules, inhibitors of DHFR, with interesting and potentially selective antibacterial properties.

Key words: dihydrofolate reductase, docking, inhibitors, pyrimido[4,5-*d*]pyrimidine-2,4-diamine, structure-activity relationship

Introduction

Dihydrofolate reductase or DHFR (EC 1.5.1.3.) catalyzes NADPH-dependent reduction of 7,8-dihydrofolate to 5,6,7,8-tetrahydrofolate (*1,2*), thus producing an important cofactor for a number of one carbon transfer reactions and is essential for the biosynthesis of purines, pyrimidines and amino acids (*3*). Inhibition of DHFR activity leads to a deficiency of thymidylate (dTMP), thus causing inhibition of cell growth (*4–6*).

DHFR is an enzyme of a great importance in metabolic pathways of the majority of both prokaryotic and eukaryotic organisms. In contrast to microbial DHFRs, mammalian DHFRs are highly conserved (*7*). Although human and bacterial DHFR share only 26 % sequence identity, overall 3D-structure of the proteins is rather similar (*7*). The difference in the primary structure of human DHFR and DHFRs from other species allows the selective inhibition of the pathogen growth with adequate inhibitors (*6*) without detrimental effects to the human cells. On the other hand, some DHFR inhibitors are used in therapy of non-infective human diseases like psoriasis, inflammatory bowel disease, rheumatoid arthritis and neoplastic diseases (*3*).

The majority of DHFR inhibitors which are currently in use or being under investigation are derivates of folic acid having 2,4-diamino substitution in pyrimidine ring and structurally belong to different classes (pyrimidines, pteridines, quinazolines, pyrido-pyrimidines) (*1,5*) (Fig. 1). Reports on the interactions of DHFR inhibitors with the active site of DHFR from different species suggest that 2,4-diaminopyrimidine ring acquires common binding interactions through the protonated N1 and 2-amino groups (*1*).
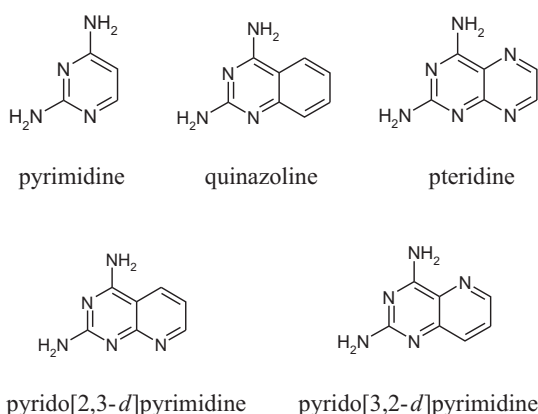

pyrimidine   quinazoline   pteridine

pyrido[2,3-*d*]pyrimidine   pyrido[3,2-*d*]pyrimidine

Fig. 1. The majority of DHFR inhibitors are derivates of folic acid. Core structures of the main classes of DHFR inhibitors containing 2,4-diamino substituted pyrimidine ring are presented

DHFR inhibitors are structurally divided in two classes – classical antifolates, which are structural analogues of folic acid bearing glutamate moiety in the distal part of the molecule, and non-classical antifolates, which are lipophilic analogues of folic acid, lacking the glutamate residue (*3,5*).

The aim of this study is to introduce pyrimido-pyrimidines as a novel class of bacterial DHFR (bDHFR) and in that way to set the basis for finding the inhibitor with improved properties compared to the currently available (trimethoprim, pyrimethamine, proguanil) or investigated (iclaprim, brodimoprim) drugs. Here 60 compounds are presented, chosen from the in-house compound library on the basis of the structural similarities to the known non-classical DHFR inhibitors. They were tested for potency and selectivity for bacterial (*Escherichia coli*) and human DHFR.

Materials and Methods

Chemicals and enzymes

All chemicals were of analytical grade and, if not stated otherwise, were purchased from Sigma (USA). Human DHFR enzyme was purchased from Sigma (USA). *E. coli* DHFR enzyme was kindly provided by J. J. Clement (Essential Therapeutics, Waltham, MA, USA).

Test compounds

The compounds structurally belonging either to pyrimido[4,5-*d*]pyrimidine-2,4-diamine or 2,4-pteridinediamine class were selected from the in-house library. In pyrimido[4,5-*d*]pyrimidine class of compounds the bridge area is composed of N-C moiety linked at the position 7, while in pteridinediamine class, there is C-N moiety at position 6. Purity of the compounds was determined to be >95 % detected by HPLC/MS. All compounds were initially dissolved in DMSO and subsequently diluted with the culture medium to the final concentration prior to use.

DHFR activity assay

The method used to determine DHFR activity was modified according to the standard one (*8*). Briefly, the enzyme activity was measured by monitoring the absorbance at 340 nm of the reaction mixture containing 20 nM DHFR, the tested compound (in the concentrations ranging from 0.1 nM up to 100 µM), dihydrofolic acid 100 µM, NADPH 200 µM, and mercaptoethanol 5 mM in Hepes buffer 100 mM, pH=7.0, at 37 °C. The concentrations of the test compound required to reduce DHFR activity by 50 % (IC_{50}) were determined by semilogarithmic plots of the data yielding normal sigmoidal curves using GraphPad Prism (v. 4.0 for Windows; GraphPad Software Inc., San Diego, CA, USA).

Bacteria and cell line culture

E. coli IMPA and *E. coli* ET003 were kindly provided by J. J. Clement (Essential Therapeutics, USA). *E. coli* IMPA strain (imp4213::tn10) (*9*) is a highly permeable strain of *E. coli* MG1655 (*10*). *E. coli* ET003 is highly permeable strain of *E. coli* LH18 strain, which is *dhfr*⁻ strain of *E. coli* MG1655. *E. coli* ET003 strain was made using parent strain *E. coli* LH18 (*11*) and transduced using P1 lysate made on *E. coli* IMPA (imp4213::tn10). Bacteria were grown in Luria Bertani (LB) medium, under the standard conditions.

Human acute monocytic leukemia cell line THP-1 (ATTC TIB-202) was obtained from ATCC (Manassas, VA, USA) and asynchronously grown (37 °C, 5 % CO_2, relative humidity 5 %) in RPMI 1640 medium supplemented with fetal bovine serum (10 %), penicillin G (100 U/mL), streptomycin-sulphate (100 µg/mL), amphotericin B (250 ng/mL) and plasmocin (2.5 µg/mL) (all purchased from Gibco, Grand Island, NY, USA).

MIC determination

Microdilution MIC (minimal inhibitory concentration) determination was performed as recommended by the National Committee for Clinical Laboratory Standards (NCCLS) (*12*). The growth inhibitory properties of the test compounds were determined by a twofold serial dilution method – for each compound the series of the solutions whose concentrations differed by a factor of two were prepared, to each solution a fixed amount of the previously prepared test culture was added and the mixture was incubated at 37 °C overnight. Antibacterial activity of each compound was expressed as its MIC, *i.e.* the lowest concentration that just inhibited bacterial growth. Each concentration of the compounds was tested in duplicate and in two independent experiments.

Proliferation assay

Cell proliferation assay was performed using Cell-Titer 96®AQ$_{ueous}$ One Solution Cell Proliferation Assay (Promega) (*13*). THP-1 cells ($5 \cdot 10^4$ cells/well) were placed into 96-well flat bottom microtiter plate in a final volume of 100 µL of the medium containing test compounds in the concentrations ranging from 0.1 nM up to 100 µM. After 72 hours of cultivation under standard conditions, 20 µL of MTS were added into the medium and cells were additionally incubated in the dark at 37 °C for the next 2 hours for colour development. The absorbance was read at the wavelength of 490 nm using the microplate reader Victor2-1420 Multilabel Counter (PerkinElmer, Wellesley, MA, USA). Two independent experiments were performed. The results were expressed as EC$_{50}$ values (the compound concentration that efficiently inhibited cell growth by 50 %), determined with GraphPad Prism (v. 4.0 for Windows; GraphPad Software Inc., San Diego, CA, USA) from semilogarithmic plots of the data yielding normal sigmoidal curves.

Docking study

Two-dimensional structures of all test compounds were transformed into three-dimensional starting conformations for MOE (molecular operating environment; Chemical Computing Group) using MMFF94 force field. The protonation was adjusted to allow optimal interactions with the protein active site. Crystal structures of both, bDHFR cocrystalized with methotrexate (MTX) (deposited in Protein Data Bank (PDB) as 1RA3) (*14*) and hDHFR cocrystalized with LIH (6-([5-quinolylamino]-methyl)-2,4-diamino-5-methylpyrido[2,3-*d*]pyrimidine), a lypophilic antifolate (deposited in PDB as 1KMS) (*15*), were used for molecular docking. GOLD (*16*) was also used for molecular docking, as well as Goldscore fitness function for ranking of the solutions. MOE 2006.08 and GOLD 3.2 were used with default fitness function parameters and default GA options (population size 100, no. of islands 5, no. of operations 100 000). Heavy atom root mean square deviation (RMSD) between the crystal and the best docked structure was 4.2 calculated by smart_rms utility provided as part of GOLD package.

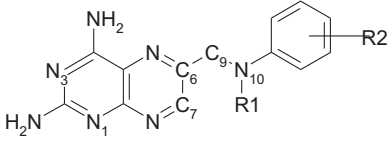*Molecular dynamics simulations*

The 3D structures of human and bacterial DHFR were taken from the PDB; 1KMS and 1RA3, respectively, and their complexes with **24** were prepared by overlying a low energy conformation of **24** with methotrexate in 1RA3 (*14*) and LIH in 1KMS (*15*). The complexes were completed by the addition of all hydrogen atoms. According to the experimental conditions, all Asp and Glu were negatively charged and all Lys and Arg were positively charged. Histidines were neutral and their protonation site (either N$_\delta$ or N$_\epsilon$) was determined according to their neighborhood and probability of H-bond formation. For the purpose of complex simulation within the program suite Amber, ligands were parameterized with the gaff force field (*17*), and charges and missing parameters were determined using the modules Antechamber and Parmcheck. Energy minimization and molecular dynamics (MD) simulations were performed with the Sander modules of the Amber10 package (*18*) using the ff03 force field (*19*). Simulations were performed in explicit solvent (TIP3P water type was used) (*20*) using periodic boundary conditions with a truncated octahedron as a unit cell. The complex 1KMS-**24** was neutral (*i.e.* protein contained equal number of positively and negatively charged amino acid residues, 25 of each), while to assure neutrality of the 1RA3-**24** system, 11 Na$^+$ ions were added. The long-range electrostatic interactions were evaluated using Particle Mesh Ewald (PME) method (*21*) with cutoff radius of 11 Å for calculating the real part contributions to electrostatic and van der Waals interactions. The system was optimized before applying MD simulations. Energy minimization was accomplished in three steps: in the first two, the protein-backbone atoms were restrained to the initial position with a harmonic forces of 19 kcal/(mol·Å) and 1 kcal/(mol·Å), respectively, and water molecules and substrate were relaxed. In the third step, the whole system was unrestrained. The time step used during MD simulation was 1 fs. The equilibration was performed in two steps: heating and density adjustment. The heating-up MD simulations (temperature increasing from 0 to 300 K during 20 ps) were performed at constant volume with the protein backbone atoms restrained with a harmonic force of 9 kcal/(mol·Å). Density was adjusted for another 20 ps of MD simulations at constant pressure (restraints as in the previous step). MD production runs were carried out at 300 K for 100 ps. Temperature was controlled by Langevin dynamics with a collision frequency of 1 ps^{-1}.

Results and Discussion

The substances tested in this study were selected from the available in-house compound library on the basis of their structural resemblance to the known non-classi-

Table 1. Structures of the tested 2,4-pteridinediamine derivates

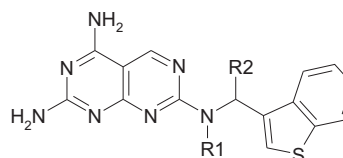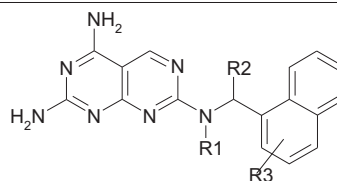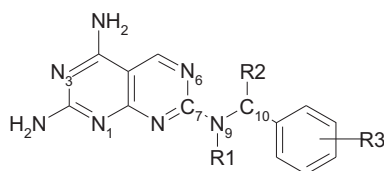| Compound no.	R1	R2
1	H	–
2	CH$_3$	–
3	CH$_2$CH$_3$	–
4	CH$_2$CH$_2$CH$_3$	–
5	CH$_2$CHCH$_2$	–
6	CH$_2$CH$_2$CH$_2$CH$_3$	–
7	CH(CH$_3$)$_2$	–
8	H	3 CHOHCH$_3$
9	H	4 OCH$_2$CH$_3$
10	H	4 NH$_2$
11	H	3 NO$_2$
12	CH$_3$	3 NO$_2$
13	CH$_3$	4 COOH
14	CH$_3$	4 COOCH$_3$
15	H	3,4 C$_3$H$_4$
16	H	2,3 C$_4$H$_4$
17	H	3,4 C$_4$H$_4$
18	H	2,3 C$_4$H$_3$4Cl

cal DHFR inhibitors. Structurally the substances belong to two classes: the first one comprises compounds having pteridine ring (Table 1), while the second one comprises those with pyrimido-pyrimidine ring (Table 2). Some pteridine compounds are well-known DHFR inhibitors, while pyrimido-pyrimidines have not yet been described in literature as DHFR inhibitors. This is why different representatives of this structural class have been chosen for this study, and then it was searched for pteridine substances that were structurally similar to the chosen pyrimido-pyrimidines. Different phenyl or naphthyl derivates were linked to these ring structures by a bridge moiety. In pteridine class the bridge moiety (C-N) was attached at position 6, while in pyrimido-pyrimidines the bridge (N-C) was at position 7, since saturated nitrogen atom was at position 6. Additionally, the major-

ity of pyrimido-pyrimidine derivates had both atoms in the bridge area substituted, while C atom in the bridge area of pteridine derivates was not substituted.
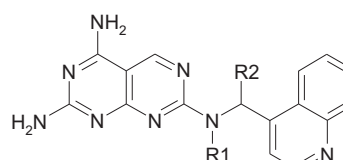
The efficacy and the specificity of the compounds as inhibitors of DHFR were tested in inhibition assays using bacterial (*E. coli*; bDHFR) and human (hDHFR) enzyme, while their growth inhibition properties were determined using highly permeable strain of *E. coli* and its *dhfr* knockout isostrain, and THP-1 cell line, as an eukaryotic model. The obtained results expressed as IC_{50} values (μM) for the inhibition of the enzymes, as MIC values (μg/mL) for bacterial growth inhibition and as EC_{50} values (μM) for THP-1 proliferation inhibition are presented in Table 3. In all assays, methotrexate (MTX), a potent inhibitor of both bDHFR (IC_{50}=5 nM) and hDHFR (IC_{50}=

Table 2. The structures of the tested pyrimido[4,5-*d*]pyrimidine-2,4-diamine derivates

Compd. no.	R1	R2	R3
19	CH_3	H	–
20	CH_2CH_3	H	4 CH_3
21	CH_3	CH_3	–
22	CH_3	CH_3	$4CH_2OH$
23	CH_3	H	2,3 C_4H_4
24	CH_3	CH_3	2,3 C_4H_4
25	CH_3	CH_2OH	2,3 C_4H_4
26	CH_2CH_3	CH_3	2,3 C_4H_4
27	CH_2CH_3	CH_3	3,4 C_4H_4
28	CH_2CH_2OH	CH_3	2,3 C_4H_4
29	CH_2COOH	CH_3	2,3 C_4H_4
30	$CH_2CH_2CH_3$	CH_3	2,3 C_4H_4
31	CH_2CHCH_2	CH_3	2,3 C_4H_4
32	CH_2CH_2COOH	CH_3	2,3 C_4H_4
33	$CH_2CH_2NH_2$	CH_3	2,3 C_4H_4
34	$CHCH_2CH_2$	CH_3	3,4 C_4H_4
35	$CH_2CHCH_2CH_2$	CH_3	2,3 C_4H_4
36	$CH_2CH_2CH_2CH_3$	CH_3	2,3 C_4H_4
37	$CH_2CH_2CH_2COOH$	CH_3	2,3 C_4H_4
38	$CH_2CH_2CH_2CH_2CH_3$	CH_3	2,3 C_4H_4
39	$CH_2CH_2CH_2CH_2NH_2$	CH_3	2,3 C_4H_4
40	$CH_2CH_2CH_2CH_2CH_2NH_2$	CH_3	2,3 C_4H_4
41	$CH_2CH_2OCH_2CH_3$	CH_3	2,3 C_4H_4
42	$CH_2CH_2OCH_2CH_2CH_3$	CH_3	2,3 C_4H_4
43	$CH_2CH_2OCH_2CH_2OH$	CH_3	2,3 C_4H_4
44	$CH_2CH_2CH_2OCH_2CH_3$	CH_3	2,3 C_4H_4
45	$CH_2(CH_2)_2OCH_2CH(CH_3)_2$	CH_3	2,3 C_4H_4
46	$CH_2C_6H_5$	CH_3	2,3 C_4H_4
47	$CH_2CH_2C_6H_9$	CH_3	2,3 C_4H_4
48	$CH_2CH_2C_6H_4F$	CH_3	2,3 C_4H_4
49	$CH_2CH_2CH_2C_3N_2H_2CH_3$	CH_3	2,3 C_4H_4

Compd. no.	R1	R2	R3
50	CH_3	CH_3	$4CH_3$
51	CH_2CH_3	CH_3	$4CH_3$
52	$CH_2CHCH_2CH_2$	CH_3	$4CH_3$
53	$CH_2CHCH_2CH_2$	CH_3	$4Cl$
54	CH_3	CH_3	$2CH_2CH_3$
55	CH_3	H	$2OCH_2CH_3$
56	CH_2CH_2COOH	H	$2OCH_2CH_3$

Compd. no.	R1	R2
57	CH_3	CH_3
58	CH_2CH_3	CH_3
59	$CH_2CHCH_2CH_2$	CH_3

Compd. no.	R1	R2
60	CH_3	CH_3

Table 3. The experimental results of the tested compounds (expressed as IC_{50}, MIC and EC_{50} values)

Compd. no.	bDHFR IC_{50} /μM	*E. coli* IMPA MIC/(μg/mL)	hDHFR IC_{50} /μM	THP-1 EC_{50} /μM	Select. ratio	Compd. no.	bDHFR IC_{50} /μM	*E. coli* IMPA MIC/(μg/mL)	hDHFR IC_{50} /μM	THP-1 EC_{50} /μM	Select. ratio
1	2.2	4	4.6	23.3	2.09	32	0.93	>64	22	>100	23.66
2	n/a	1	n/a	n/a	n/a	33	2	2	>100	>100	–
3	0.11	0.5	n/a	n/a	n/a	34	4	4	15	13.7	3.33
4	0.15	0.125	1.6	1.6	10.67	35	0.6	0.5	8	10.3	13.33
5	0.15	0.125	2.0	6.2	13.33	36	1.84	2	4	39.6	2.17
6	0.6	0.5	1.7	2.6	2.83	37	2.73	>64	19.1	87.6	7.00
7	0.88	0.5	0.8	3.1	0.91	38	1.85	2	9	12.9	4.86
8	19	>64	>100	74.1	0.26	39	4.8	8	2.8	93	0.58
9	14	32	16	31.1	1.14	40	3	4	3.9	36.5	1.30
10	>100	>64	14	>100	–	41	1	1	4.9	32.6	4.90
11	n/a	2	n/a	n/a	n/a	42	3.3	4	29.4	19.1	8.91
12	n/a	0.125	n/a	n/a	n/a	43	1.7	2	10.1	28.7	5.94
13	0.2	64	n/a	>100	n/a	44	3.5	4	32.6	32.6	9.31
14	2.2	2	0.3	19.1	0.15	45	3.4	4	34	12.7	10.00
15	>100	>64	n/a	35.6	n/a	46	0.88	1	13	14.4	14.77
16	11	16	0.5	32	0.05	47	2.5	2	7.8	12.7	3.12
17	48	64	21	>100	0.44	48	1.03	0.5	12.5	14.4	12.14
18	0.6	0.5	0.5	2.7	0.83	49	0.8	1	12.4	34.9	15.50
19	35.7	>64	82	>100	2.30	50	0.055	0.125	0.85	6	15.45
20	21.4	>64	n/a	n/a	n/a	51	0.21	0.25	1	5.2	4.76
21	11.2	16	9	>100	0.80	52	3.5	4	12.5	11.6	3.57
22	6.8	16	90.5	>100	0.08	53	2.2	2	12.5	8.1	5.68
23	3.5	4	9	33.8	2.57	54	3	8	27.8	5.4	9.27
24	**0.016**	**0.125**	**16**	**22**	**1000.00**	55	1.1	0.5	0.98	3.4	0.89
25	76	>64	14.1	108	0.19	56	8.3	>64	13.6	>100	1.64
26	0.2	0.25	17	11.6	85.00	57	0.05	0.125	2	15.9	40.00
27	3.2	4	33	22.9	10.31	58	0.15	0.125	2	5.7	13.33
28	0.3	0.25	13.3	18.5	44.33	59	0.27	0.25	1	5.2	3.70
29	21	>64	59.2	>100	2.82	60	0.7	0.5	8.8	33.4	12.57
30	0.96	0.5	15	18	15.63	MTX	0.005	>64	0.001	0.01	0.20
31	0.4	0.5	15	13.7	37.50	TMP	0.010	0.125	>100	>100	–

n/a – data not available

=1 nM) that inhibits only the growth of eukaryotic cell (EC_{50}=10 nM), and trimethoprim (TMP), a selective inhibitor of bacterial enzyme (IC_{50}=10 nM) and bacterial growth (MIC<0.125 μg/mL), were used as standard compounds (Fig. 2).

The main structural differences among the compounds within pteridine class arose from the moieties attached to the nitrogen atom (N10) in the bridge area, which were designated as R1, and the moieties attached to phenyl linked to the nitrogen atom (N10), which were designated as R2. Structurally the simplest compound (**1**) within this class, bearing hydrogen as R1, showed IC_{50} values in low micromolar range, 2.2 and 4.6 μM for

bDHFR and hDHFR, respectively. Introduction of methyl group (**2**) instead of hydrogen as R1 increased antibacterial potency of the compound four times, while the extension of the moiety up to three carbon atoms (**4**), caused an increase up to 20 times (IC_{50} 0.15 μM and MIC 0.125 μg/mL), which implies an enhancement of the interactions of R1 groups with atoms in the active site of bDHFR. However, further elongation of R1 moiety (**6**) resulted in fourfold decrease of antibacterial activity. These data suggest that the optimal number of carbon atom units at this position is three or less. It was previously shown that alkylation of N10 in pyrido-pyrimidines (*22,23*) causes tenfold increase of their inhibitory effects toward hDHFR and it was suggested that
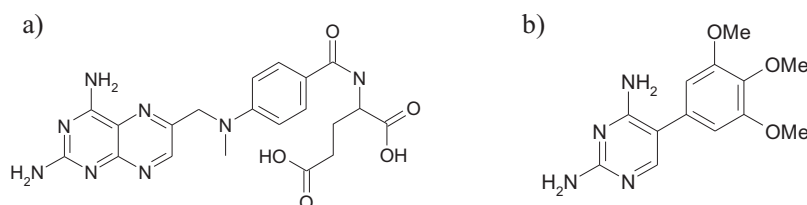

Fig. 2. Structures of: a) methotrexate (MTX) and b) trimethoprim (TMP)

N10 substitutions serve to partially restrain the conformational flexibility, thus probably providing additional interactions with the enzyme. However, according to another hypothesis, N10 alkylation has little or no effect on hDHFR inhibition, but affects transport of the compounds into the cells (*24*). The modifications of phenyl group at N10 position in pteridine class caused different effects, *e.g.* the attachment of amino group (**10**) completely abolished antibacterial activity, while the introduction of nitro group (**11**, **12**) caused slight increase of the activity (2- to 8-fold) compared to the compound with just phenyl moiety (**1**, **2**). These data suggest the importance of electron-withdrawing group at this position, probably due to the interactions with amino acid residues in the active site of bDHFR enzyme. On the other hand, the attachment of carboxyl group (**13**) did not affect bDHFR inhibition ability, but it resulted in the loss of antibacterial activity. Esterification of this acidic group (**14**) led to 10 times reduced bDHFR inhibition, but interestingly, antibacterial property was restored. Since similar effect was also observed in THP-1 cells, these findings suggest the importance of negatively charged group in disabling the entrance of the compounds into the cell. The presence of phenyl group attached to N10 (**1**) is favourable compared to α-linked naphthyl (**16**) for the bDHFR inhibition (phenyl derivate was 5 times more potent than naphthyl); however, the effect was reversed in the case of hDHFR, where phenyl derivate was 8 times less potent than the naphthyl one. The beneficial effect of naphthyl *vs.* phenyl moiety for hDHFR inhibition was also described for other structurally related compounds (quinazolines (*25*), pyrido-pyrimidines (*26*) or deazaaminopterin derivates (*24*)), which is in accordance with the findings that hDHFR active site is larger than the active site in the bacterial enzyme. The positioning of naphthyl moiety seems to be of importance since the β-naphthyl derivate (**17**) showed 5 and 40 times decrease of bDHFR and hDHFR activity, respectively, when compared to the α-naphthyl one (**16**). The importance of naphthyl moiety positioning was also observed in the case of both, pyrido-pyrimidines (*24–26*) and 2,4-diamino-8-deazafolate analogues.

To be able to compare the selectivity of the compound for bacterial *vs.* human enzyme, the ratio of IC_{50} values of bDHFR and hDHFR was calculated. Within pteridine class none of the test compounds showed significant selectivity since the ratio was mainly between 0.1 and 10.

For all tested pteridine derivates, docking simulations predicted the same binding mode for both bDHFR and hDHFR as for methotrexate. The highest scored compound (Table 4) for bDHFR activity was the one with carboxyl moiety attached to phenyl group (**13**), while structurally the simplest one in this class (**1**) had the smallest scores for both bDHFR and hDHFR. Alkylation of N10 was recognized to be preferred for the inhibition of both enzymes. However, the results of docking studies did not correlate with IC_{50} for bDHFR and recognized neither different effects of phenyl and naphthyl group attached to N10 nor the influence of naphthyl positioning on the inhibition of both enzymes.

Structural differences among the tested compounds belonging to pyrimido-pyrimidine class arose from the diversities of substituents on nitrogen atom at position 9 (N9) in the bridge area, designated as R1, on carbon atom at position 10 (C10), designated as R2, and substituents positioned on phenyl or naphthyl moiety (attached) at position C10, designated as R3 (Table 2). Few compounds bearing cyclic moieties different than phenyl or naphthyl at C10, chosen in order to estimate the importance of specific cyclic moiety at that particular position, were also tested. Among the tested pyrimido-pyrimidines, the only compound bearing hydrogen as R3 on the phenyl moiety (**21**), which showed moderate inhibition of both bDHFR (11 μM) and hDHFR (9 μM), had methyl groups as both R1 and R2, while the compound lacking methyl moiety at the position C10 (**19**) showed higher IC_{50} for both bDHFR (35.7 μM) and hDHFR (82 μM). Similar effects were also observed in the case of pyrido-pyrimidine DHFR inhibitors, where methylation at the position N9 caused 15–40 times increase of hDHFR inhibition (*26*). Taken together, these data suggest the importance of small groups as substituents on the atoms in the bridge moiety of these compounds for their activity as inhibitors of DHFR.

The compounds bearing naphthyl instead of phenyl moiety showed strong inhibition of bDHFR (10 to 1000 times more active compared to those with phenyl group), and interestingly, the most active one (**24**) also had methyl groups as both R1 and R2, showing bDHFR inhibition comparable to both trimethoprim and methotrexate (IC_{50}=0.016 μM). Since it exhibited moderate hDHFR inhibition (IC_{50}=24.7 μM), the selectivity ratio was calculated to be approx. 1000. Among all the tested compounds, this one had the most potent antibacterial properties (MIC=0.125 μg/mL). Like in pteridine class, the positioning of naphthyl moiety seemed to be of importance since 10 times decrease of IC_{50} values for bDHFR and 2 to 3 times decrease of IC_{50} values for hDHFR occurred when β (**27**) was shifted to α-position (**26**). The elongation of R1 to up to four carbon atoms (**36**) correlated with a decrease of inhibitory effects for bDHFR (IC_{50} dropped from 0.016 to 2 μM). However, further elongation did not cause additional change of bDHFR inhibition and it seems that N9 substitution may tolerate even larger groups like phenyl (**46**) or phenyl derivates, without affecting activity of the compound. In general, hDHFR inhibition was not very dependent on the size of R1 moiety. The introduction of carboxyl group as part of R1 (**32**, **37**) did not affect bDHFR inhibition, but at the same time it caused the loss of antibacterial activity. This phenomenon was independent of the length of alkyl chain and it suggested that the presence of negative charge has no influence on enzyme activity but strongly influences the entrance of the compounds into bacterial cell. Similar effect was also observed in the case of hDHFR and THP-1 growth inhibition.

Growth inhibition of *E. coli* lacking DHFR (ET003 strain, *dhfr⁻*) was induced with the compounds bearing two or three carbon moieties as R1 and to a smaller extent in the case of four carbon moieties (Table 5). The cyclopropyl moiety as part of R1 seemed to be prerequisite for non-bDHFR antibacterial activity since 5 different compounds (**34**, **35**, **52**, **53**, **59**) bearing this moiety showed antibacterial activity for the strain lacking DHFR.

Table 4. Docking scores of the tested compounds for bDHFR and hDHFR compared to the IC$_{50}$ values

Compd. no.	bDHFR		hDHFR		Compd. no.	bDHFR		hDHFR	
	IC$_{50}$/μM	Dock. scores	IC$_{50}$/μM	Dock. scores		IC$_{50}$/μM	Dock. scores	IC$_{50}$/μM	Dock. scores
1	2.2	54.9	4.6	65.16	32	0.93	69.54	22	82.09
2	n/a	68.29	n/a	81.3	33	2	68.91	>100	70.9
3	0.11	67.99	n/a	83.36	34	4	58.38	15	76.10
4	0.15	69.95	1.6	80.78	35	0.6	63.03	8	72.09
5	0.15	61.69	2.0	72.21	36	1.84	69.23	4	67.85
6	0.6	74.8	1.7	85.06	37	2.73	70.16	19.1	86.20
7	0.88	69.38	0.8	80.49	38	1.85	68.34	9	69.97
8	19	73.98	>100	77.79	39	4.8	71.88	2.8	73.87
9	14	69.41	16	76.5	40	3	70.39	3.9	69.27
10	>100	65	14	77.26	41	1	71.9	4.9	72.94
11	n/a	58.31	n/a	67.66	42	3.3	74.94	29.4	72.64
12	n/a	71.12	n/a	75.82	43	1.7	70.96	10.1	70.89
13	0.2	76.32	n/a	82.77	44	3.5	57.34	32.6	75.09
14	2.2	71.21	0.3	85.36	45	3.4	74	34	70.01
15	>100	60.57	n/a	70.87	46	0.88	65.08	13	76.87
16	11	57.46	0.5	69.04	47	2.5	75.75	7.8	76.48
17	48	62.02	21	73.18	48	1.03	80.87	12.5	85.01
18	0.6	59.14	0.5	74.53	49	0.8	83.19	12.4	81.03
19	35.7	62.84	82	66.17	50	0.055	61.74	0.85	73.4
20	21.4	52.12	n/a	63.79	51	0.21	64.62	1	68.5
21	11.2	57.69	9	65.94	52	3.5	71.96	12.5	73.97
22	6.8	67.98	90.5	68.48	53	2.2	68.86	12.5	75.79
23	3.5	57.15	9	69.78	54	3	58.43	27.8	70.52
24	0.016	58.92	16	68.65	55	1.1	67.02	0.98	81.82
25	76	66.52	14.1	69.87	56	8.3	69.35	13.6	84.01
26	0.2	55.2	17	69.65	57	0.05	59.9	2	78.45
27	3.2	56.61	33	71.31	58	0.15	69.8	2	74.6
28	0.3	68.54	13.3	65.34	59	0.27	75.04	1	80.27
29	21	71.43	59.2	85.22	60	0.7	63.13	8.8	64.51
30	0.96	61.78	15	74.08	MTX	0.005	95.88	0.001	109.78
31	0.4	71.7	15	74.36	TMP	0.010		>100	

n/a – data not available

Table 5. Minimal inhibitory concentration (MIC) values of the chosen pyrimido-pyrimidines for wild type *E. coli* IMPA and its *dhfr* knockout isostrain (*dhfr⁻*)

Compd. no.	MIC/(μg/mL)	
	E. coli IMPA	*E. coli dhfr⁻*
26	0.25	16
27	4	16
30	0.5	16
31	0.5	16
33	2	2
34	4	4
35	0.5	8
36	2	16
40	4	16
51	0.25	16
52	4	8
53	2	4
54	8	8
58	0.125	16
59	0.25	8

All this suggests that size and spatial positioning of R1 substituents might be important for achieving interactions with some targets other than DHFR or for mechanisms of unspecified toxicity.

The presence of cyclic structures (**57, 58, 59, 60**) similar to naphthyl moiety at position C10 caused no significant change of inhibitory properties of the compounds, suggesting the importance of the moiety size at this position. On the other hand, introduction of various substituents on naphthyl moiety resulted in different effects depending on substituent positioning and character. For some more general conclusion, more compounds with minimal structural differences on naphthyl moiety should be tested.

Within pyrimido-pyrimidine class, 6 compounds (**24, 26, 28, 31, 32, 57**) with high selectivity ratio were recognized. In general, the selectivity was primarily due to a high potency of the compounds to inhibit bDHFR activity, while the ability to inhibit hDHFR was not influenced significantly. These compounds share some structural similarities in having groups up to three atoms as R1, methyl moiety as R2 and naphthyl (or benzo(b)thiophenyl – **57**) attached to C10. Even a smallest

modification of these structural motifs led to a decrease of bDHFR inhibition and consequently to the loss of selectivity. Similar effect was observed when any of discriminating motifs was missing, so it seems that high selectivity is strongly related to relative narrow structural motif identity.

The results of docking study (Table 4) were compared to the compound structures and some relations with the compound activities were observed. Docking scores for both enzymes were higher for compounds with bigger group attached to N9 position. In the case of both DHFRs, but especially of hDHFR, the presence of carboxyl group (**32, 37**) correlated with higher docking values, suggesting the importance of negatively charged groups. However, docking results did not reflect the influence of N9 methylation on the activity, the differences that arose from the presence of phenyl *vs.* naphthyl moiety attached to the position 10, as well as the effects of naphthyl moiety positioning. It seems that for both bDHFR and hDHFR the docking scoring did not have predictive impact, since the corresponding scores were not in significant correlation with the results of *in vitro* study (IC$_{50}$).

In order to rationalize reasons for high potency and remarkable selectivity of compound **24** towards bDHFR inhibition, the bDHFR-**24** and hDHFR-**24** complexes were subjected to molecular dynamics (MD) simulations. For this purpose the energy-minimized conformation of **24** was overlaid with methotrexate in the active site of bDHFR, with LIH in the active site of hDHFR (Fig. 3) (see Methods) and the complexes were solvated, neutralized and relaxed. During MD simulations, hydrogen bonds, either direct or water-mediated, between the compound **24** and D27, I5, I94 and Y100 in the active site of bDHFR were formed (Fig. 4), which are the same amino acid residues as those that interact with methotrexate in the crystal structure (1RA3). Interaction between **24** and hDHFR was established through the H-bonds with E30, I7 and L22, *i.e.* with some of the amino acid residues LIH interacts as well. Although MD simulations did not show substantial difference between **24** bindings to the active site of the two enzymes, it revealed slightly larger number of H-bonds formed between **24** and bDHFR than between **24** and hDHFR. However, it should be stressed that the simulations were quite short.

hDHFR is a neutral molecule at physiological conditions unlike highly negatively charged bDHFR and it might be possible that favourable electrostatic forces are one of the reasons for high affinity of compound **24** towards bDHFR. Further on, the binding site entrance is wider in bDHFR than in hDHFR, enabling easier accommodation of **24**, especially the bulky naphthyl moiety, into the bDHFR binding site than into that of hDHFR and its binding in a specific way. Nevertheless, further studies are needed for understanding the mechanism responsible for high activity and selectivity of this compound.

Conclusions

Compounds with pyrimido-pyrimidine structure as a novel class of DHFR inhibitors are proposed here. Some of them have shown promising behaviour in bDHFR in-
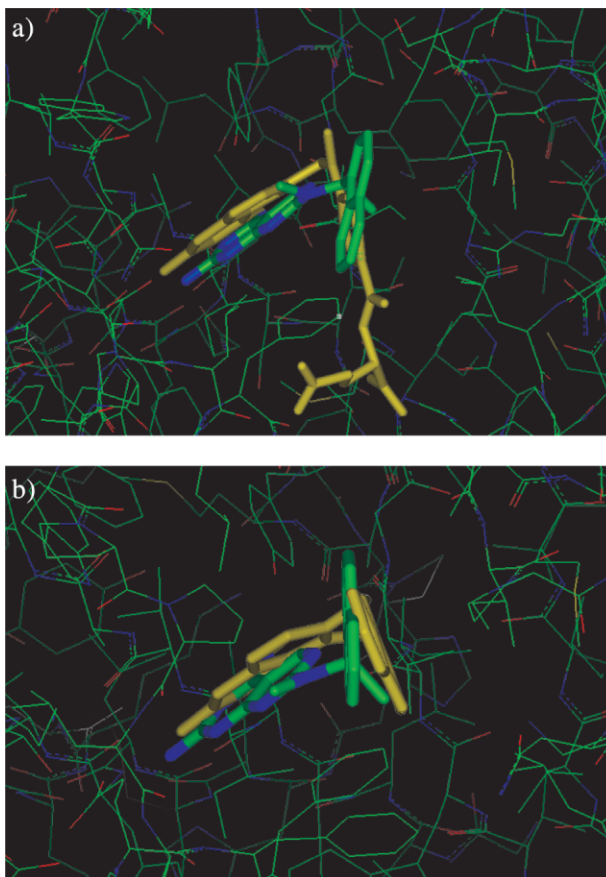

Fig. 3. Overlay of: a) compound **24** (green/blue) with methotrexate (yellow) in the bDHFR active site; b) compound **24** (green/blue) with LIH (yellow) in the hDHFR active site
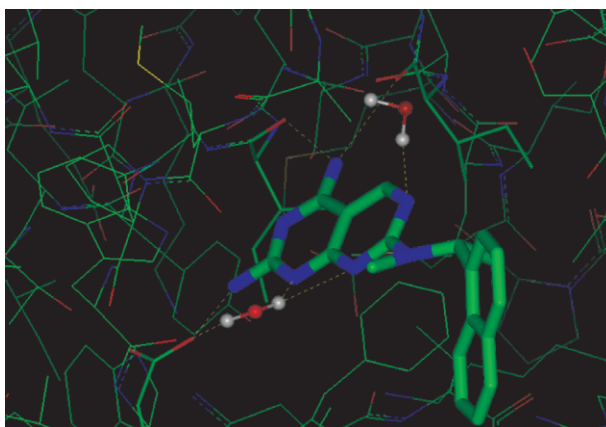

Fig. 4. Some of the hydrogen bonds between the compound **24** and bDHFR formed during 100 ps of MD simulation at room temperature. The substrate is shown as stick representation, the water molecules as ball and stick representation, and the protein amino acid residues as lines, with the amino acid residues interacting with the compound **24** by direct hydrogen bonds slightly highlighted. For the purpose of clarity only hydrogen atoms in water molecules are shown

hibition and their unique and distinctive structural preferences could be a base for selectivity towards inhibition of bacterial *vs.* human enzyme.

Screening results suggest a high importance of the group size linked to the atoms in the bridge area. The pteridine class of the compounds favours up to three--atom group linked to nitrogen atom in the bridge moiety, while pyrimido-pyrimidines prefer just methyl group for bDHFR inhibition. Furthermore, in the case of pyrimido-pyrimidines, naphthyl moiety linked by the bridge area seems to be preferred over phenyl moiety for bDHFR inhibition, which is opposite to the findings for the compounds belonging to other structurally similar classes. The negatively charged group seems to be of a great importance for the entrance of the compounds belonging to both tested classes into the cell.

High selectivity of a few pyrimido-pyrimidines occurs due to a higher potency of bDHFR inhibition without effects on hDHFR inhibition. It seems that these few compounds might have the stringent structure freedom and flexibility, based on the specific combination of prerequisite structural motifs that enables them to fit into bDHFR active site in relatively specific manner. The active site of hDHFR being larger than the one of bDHFR may not have stringency to accommodate these structures, so it may not 'recognize' this unique and specific structural motif in a manner like bDHFR active site does. As a consequence, a few pyrimido-pyrimidine compounds, carrying specific combination of substituents, exhibit stronger bDHFR inhibition and consequently higher selectivity ratio.

Virtual screening of the compounds with described properties may be inconclusive in some cases; however, together with the results of experimental studies may provide better understanding of the inhibition process. Presented results will help to set the basis for designing new small molecules, inhibitors of DHFR, with interesting and potentially selective antibacterial properties.

Acknowledgements

References

1. A. Gangjee, W. Li, J. Yang, R.L. Kisliuk, Design, synthesis, and biological evaluation of classical and nonclassical 2--amino-4-oxo-5-substituted-6-methylpyrrolo[*3,2-d*]pyrimidines as dual thymidylate synthase and dihydrofolate reductase inhibitors, *J. Med. Chem. 51* (2008) 68-76.

2. J. Feng, S. Goswami, E.E. Howell, R67, the other dihydrofolate reductase: Rational design of an alternate active site configuration, *Biochemistry, 47* (2008) 555-565.

3. B.I. Schweitzer, A.P. Dicker, J.R. Bertino, Dihydrofolate reductase as a therapeutic target, *FASEB J. 4* (1990) 2441-2452.

4. A. Gangjee, H.D. Jain, S. Kurup, Recent advances in classical and non-classical antifolates as antitumor and antiopportunistic infection agents: Part I, *Anticancer Agents Med. Chem. 7* (2007) 524-542.

5. A. Gangjee, H.D. Jain, S. Kurup, Recent advances in classical and non-classical antifolates as antitumor and antiopportunistic infection agents: Part II, *Anticancer Agents Med. Chem. 8* (2008) 205-231.

6. A. Gangjee, S. Kurup, O. Namjoshi, Dihydrofolate reductase as a target for chemotherapy in parasites, *Curr. Pharm. Des. 13* (2007) 609-639.

7. I.M. Kompis, K. Islam, R.L. Then, DNA and RNA synthesis: Antifolates, *Chem. Rev. 105* (2005) 593-620.

8. J.J. Burchall, G.H. Hitchings, Inhibitor binding analysis of dihydrofolate reductases from various species, *Mol. Pharmacol. 1* (1965) 126-136.

9. B.A. Sampson, R. Misra, S.A. Benson, Identification and characterization of a new gene of *Escherichia coli* K-12 involved in outer membrane permeability, *Genetics, 122* (1989) 491-501.

10. K.F. Jensen, The *Escherichia coli* K-12 'wild types' W3110 and MG1655 have an rph frameshift mutation that leads to pyrimidine starvation due to low pyrE expression levels, *J. Bacteriol. 175* (1993) 3401-3407.

11. E.E. Howell, P.G. Foster, L.M. Foster, Construction of a dihydrofolate reductase-deficient mutant of *Escherichia coli* by gene replacement, *J. Bacteriol. 170* (1988) 3040-3045.

12. Methods for dilution antimicrobial susceptibility tests for bacteria that grow aerobically, NCCLS, M7-A7 26, Wayne, PA, USA (2003).

13. T. Mosmann, Rapid colorimetric assay for cellular growth and survival: Application to proliferation and cytotoxicity assays, *J. Immunol. Methods, 65* (1983) 55-63.

14. M.R. Sawaya, J. Kraut, Loop and subdomain movements in the mechanism of *Escherichia coli* dihydrofolate reductase: Crystallographic evidence, *Biochemistry, 36* (1997) 586-603.

15. A.E. Klon, A. Héroux, L.J. Ross, V. Pathak, C.A. Johnson, J.R. Piper, D.W. Borhani, Atomic structures of human dihydrofolate reductase complexed with NADPH and two lipophilic antifolates at 1.09 Å and 1.05 Å resolution, *J. Mol. Biol. 320* (2002) 677-693.

16. G. Jones, P. Willett, R.C. Glen, A.R. Leach, R. Taylor, Development and validation of a genetic algorithm for flexible docking, *J. Mol. Biol. 267* (1997) 727-748.

17. J. Wang, R.M. Wolf, J.W. Caldwell, P.A. Kollman, D.A. Case, Development and testing of a general Amber force field, *J. Comput. Chem. 25* (2004) 1157-1174.

18. Amber10, The Amber Molecular Dynamics Package, University of California, San Francisco, CA, USA (2008) (*http://ambermd.org*).

19. Y. Duan, C. Wu, S. Chowdhury, M.C. Lee, G. Xiong, W. Zhang, R. Yang, P. Cieplak, R. Luo, T. Lee, J. Caldwell, J. Wang, P. Kollman, A point-charge force field for molecular mechanics simulations of proteins based on condensed--phase quantum mechanical calculations, *J. Comput. Chem. 24* (2003) 1999-2012.

20. M.W. Mahoney, W.L. Jorgensen, A five-site model for liquid water and the reproduction of the density anomaly by rigid, nonpolarizable potential functions, *J. Chem. Phys. 112* (2000) 8910-8922.

21. T. Darden, D. York, L. Pedersen, Particle mesh Ewald - An NlogN method for Ewald sums in large systems, *J. Chem. Phys. 98* (1993) 10089-10092.

22. A. Gangjee, A. Vasudevan, S.F. Queener, R.L. Kisliuk, 6--substituted 2,4-diamino-5-methylpyrido[2,3-*d*]pyrimidines as inhibitors of dihydrofolate reductases from *Pneumocystis carinii* and *Toxoplasma gondii* and as antitumor agents, *J. Med. Chem. 38* (1995) 1778-1785.

23. A. Gangjee, A. Vasudevan, S.F. Queener, Synthesis and biological evaluation of nonclassical 2,4-diamino-5-methylpyrido[2,3-*d*]pyrimidines with novel side chain substituents as potential inhibitors of dihydrofolate reductases, *J. Med. Chem. 40* (1997) 479-485.

24. J.R. Piper, C.A. Johnson, C.A. Krauth, R.L. Carter, C.A. Hosmer, S.F. Queener, S.E. Borotz, E.R. Pfefferkorn, Lipo-

philic antifolates as agents against opportunistic infections. 1. Agents superior to trimetrexate and piritrexim against *Toxoplasma gondii* and *Pneumocystis carinii* in *in vitro* evaluations, *J. Med. Chem. 39* (1996) 1271-1280.

25. A. Gangjee, A.P. Vidwans, A. Vasudevan, S.F. Queener, R.L. Kisliuk, V. Cody, R. Li, N. Galitsky, J.R. Luft, W. Pangborn, Structure-based design and synthesis of lipophilic 2,4-dia-

mino-6-substituted quinazolines and their evaluation as inhibitors of dihydrofolate reductases and potential antitumor agents, *J. Med. Chem. 41* (1998) 3426-3434.

26. A. Gangjee, A. Vasudevan, S.F. Queener, R.L. Kisliuk, 2,4--diamino-5-deaza-6-substituted pyrido[*2,3-d*]pyrimidine antifolates as potent and selective nonclassical inhibitors of dihydrofolate reductases, *J. Med. Chem. 39* (1996) 1438-1446.